MOLECULAR AND CELLULAR BIOLOGY, June 1998, p. 3321–3329 Vol. 18, No. 6
0270-7306/98/$04.00+0

Mutations in the Extracellular Domain Cause RET Loss of Function by a Dominant Negative Mechanism

MARIA PIA COSMA,[1] MONICA CARDONE,[1] FRANCESCA CARLOMAGNO,[2] AND VITTORIO COLANTUONI[1,3]*

Dipartimento di Biochimica e Biotecnologie Mediche and Centro di Ingegneria Genetica, CEINGE,[1] and Centro di Endocrinologia e Oncologia Sperimentale del CNR, Dipartimento di Biologia e Patologia Cellulare e Molecolare, Facoltà di Medicina e Chirurgia, Università di Napoli "Federico II,"[2] Naples, and Facoltà di Farmacia, Università di Reggio Calabria, Catanzaro,[3] Italy

Received 26 February 1998/Accepted 19 March 1998

The *RET* proto-oncogene encodes a tyrosine kinase receptor expressed in neuroectoderm-derived cells. Mutations in specific regions of the gene are responsible for the tumor syndromes multiple endocrine neoplasia types 2A and 2B (MEN 2A and 2B), while mutations along the entire gene are involved in a developmental disorder of the gastrointestinal tract, Hirschsprung's disease (HSCR disease). Two mutants in the extracellular domain of RET, one associated with HSCR disease and one carrying a flag epitope, were analyzed to investigate the impact of the mutations on RET function. Both mutants were impeded in their maturation, resulting in the lack of the 170-kDa mature form and the accumulation of the 150-kDa immature form in the endoplasmic reticulum. Although not exposed on the cell surface, the 150-kDa species formed dimers and aggregates; this was more pronounced in a double mutant bearing a MEN 2A mutation. Tyrosine phosphorylation and the transactivation potential were drastically reduced in single and double mutants. Finally, in cotransfection experiments both mutants exerted a dominant negative effect over proto*RET* and *RET*2A through the formation of a heteromeric complex that prevents their maturation and function. These results suggest that HSCR mutations in the extracellular region cause RET loss of function through a dominant negative mechanism.

The *RET* proto-oncogene encodes a membrane receptor that expresses tyrosine kinase activity in tissues of neural crest origin, including the sympathetic ganglia, the adrenal medulla, thyroid C cells, and the excretory system of the developing kidney (3, 24, 35, 36). It is also expressed in tumors originating from neural crest cells, e.g., neuroblastoma, pheochromocytoma, and thyroid medullary carcinoma (16, 23, 30).

The RET protein shows some structural features that are homologous with the extracellular domains of cadherins, including putative Ca^{2+} binding sites. These repeats are followed by a unique cysteine-rich tract and a transmembrane segment. The intracellular region is formed by a bipartite tyrosine kinase functional domain (35, 36). Glial-cell-line-derived neurotrophic factor (GDNF) and neurturin have recently been shown to be RET ligands (5, 11, 18, 19). GDNF-deficient mice, in fact, lacked the enteric nervous system and had abnormalities in the developing kidney similar to those observed in *RET* knockout mice (29, 33, 39). Finally, GDNF and neurturin activate RET through intermediate receptors, GDNF receptors α and β. This is a growing family of proteins, anchored through a glycosylphosphatidylinositol (GPI) moiety on the surfaces of the target cells, that interact with the proper ligands and induce RET dimerization and activation (5, 18, 19).

Mutations of the *RET* proto-oncogene have been associated with several neurochristopathies: multiple endocrine neoplasia types 2A and 2B (MEN 2A and 2B), familial medullary thyroid carcinoma (FMTC), and Hirschsprung's disease (HSCR disease) (10, 13, 15, 22, 28). MEN 2 neurochristopathies are autosomal dominant cancer syndromes: MEN 2A is characterized by medullary thyroid carcinoma (MTC), pheochromocytoma, and hyperplasia of the parathyroid glands, while MEN 2B, in addition to MTC and pheochromocytoma, is characterized by developmental abnormalities without involvement of the parathyroid glands. FMTC has MTC as the only clinical phenotype (32). Single-base-pair changes in the codons specifying one of five conserved cysteine residues in the cysteine-rich region are responsible for 85 to 90% of the MEN 2A cases and the majority of FMTC cases (13). MEN 2B is caused by a single missense mutation that involves one of the conserved amino acid residues in the tyrosine kinase domain of RET (15). In all cases, the result is a "gain of function" of RET that is believed to be the initiating event that leads to foci of hyperplasia in the target organ and, eventually, to tumor formation. The MEN 2A and MEN 2B alleles behave as dominant oncogenes in in vitro systems. The MEN 2A mutations constitutively activate the receptor through the formation of covalently linked dimers, independent of the ligand (2, 31). The MEN 2B mutation appears to change the specificities of the substrates that are phosphorylated during intracellular signalling (34).

HSCR disease is a congenital disorder of the autonomic innervation of the distal gastrointestinal tract that causes its functional obstruction and results in megacolon (26). One HSCR susceptibility locus was mapped to the pericentromeric region of chromosome 10 where *RET* was localized, and, indeed, some HSCR disease patients have partial deletions of the *RET* locus (20, 21). Some other familial or sporadic cases bear missense, nonsense, or frameshift mutations distributed along the entire gene that cause amino acid substitutions or protein truncation (1, 12, 13, 28). In all these cases the receptor is inactivated, producing a clinical picture of a loss of function. The *RET* knockout in mice causes, in fact, a lack of enteric ganglion cells of the Meissner's and Auerbach's plexuses in

* Corresponding author. Mailing address: Dipartimento di Biochimica e Biotecnologie Mediche, Facoltà di Medicina e Chirurgia, Università di Napoli, "Federico II," Via Sergio Pansini, 5, 80131 Naples I, Italy. Phone: 39 81 746 3735. Fax: 39 81 746 3074. E-mail: colantuoni@dbbm.unina.it.

homozygous animals, a clinical picture that is reminiscent of HSCR disease in humans (33). HSCR mutations of the intracellular domain of RET introduced into the RET/PTCII chimeric oncogene abolished RET's biological activity and significantly decreased its kinase activity. Moreover, they exerted a dominant negative effect on the RET/PTCII oncogene and on the "activating" MEN 2A mutation (8, 25). Mutations in the extracellular domain of RET impair the correct maturation of the receptor, its exposure on the cell surface, and its biological activity (2, 6, 17).

We have analyzed in greater depth the biochemical and biological impact of two mutations in the outermost region of the extracellular domain of RET. We demonstrate that these two *RET* mutants, one carrying a "natural" HSCR single-base-pair mutation and the other carrying a stretch of additional amino acids (Flag epitope), were hampered in the glycosylation process, were retained in the endoplasmic reticulum, and were sensitive to endoglycosidase-H (Endo-H) cleavage. Similar results were obtained with a double mutant generated by inserting the Flag epitope in the *RET*2A cDNA. The immature 150-kDa species, although not exposed on the cell surface, was able to form dimers and high-molecular-weight complexes. The phosphorylation and transactivation potential of the mutants were low compared to those of protoRET and RET2A. Finally, in cotransfection-transactivation experiments the mutants interfered with the maturation and function of the 150-kDa protoRET and RET2A species through the formation of heteromeric complexes. We suggest that HSCR mutations in the extracellular domain cause RET loss of function by exerting a dominant negative effect, i.e., inactive heterodimerization between wild-type and mutated immature proteins results in loss of function.

MATERIALS AND METHODS

Plasmid constructions. The pSG-5 expression vector was used as a recipient plasmid to clone the proto*RET* full-length cDNA as an *Eco*RI-*Hin*dIII fragment (8). A DNA fragment carrying the Cys634Arg MEN 2A mutation was obtained by reverse transcription-PCR from a MEN 2A tumor and was cloned in the same proto*RET* cDNA, as described elsewhere (8). The mutation at codon 32 associated with HSCR involves the substitution of a serine with a leucine residue and has been described previously (6). To produce the Flag mutants, a 36-bp DNA fragment coding for a polyaspartic acid epitope was cloned at a unique *Eag*I site present in the 5′ region of both proto*RET* and *RET*2A cDNA. The long*RET* expression vector carries the cDNA corresponding to the 1,114-amino-acid (aa) protein, with an extension of 51 aa with respect to the short version of the receptor (13).

Cell culture and transfections. Cos 7 cells were grown in Dulbecco's modified Eagle's medium containing 10% fetal calf serum and were transfected by the calcium phosphate coprecipitation technique (14). Cells were seeded 5 h before transfection at 10^6 per 10-cm-diameter plate. Transfections were carried out with 5 μg of DNA, a quantity that was shown not to overload the cells or to interfere with the expression of other cellular proteins (8). Cotransfection experiments were performed by introducing a fixed amount of the TRE-TK-CAT reporter plasmid and increasing amounts of proto*RET*, *RET*2A, HSCR32, proto*RET*-Flag, and *RET*2A-Flag expression vectors. Alternatively, a fixed amount of proto*RET* or *RET*2A expression constructs was cotransfected with the various *RET* mutant expression vectors at 1:1, 1:2, and 1:3 molar ratios. In transactivation-cotransfection experiments, the mutation-carrying vectors were added to the transfection mixture containing the TRE-TK-CAT plasmid as the reporter and the *RET*2A plasmid as the transactivator at 1:1, 1:2, and 1:3 molar ratios with respect to the *RET*2A vector. The same amount of DNA and the same molar ratios of the mutant forms were employed with the long*RET* expression vector. Forty-eight hours after transfection, cells were lysed in a solution of 66 mM HEPES (pH 7.4), 200 mM NaCl, 1% glycerol, 1% Triton X-100, 2 mM $MgCl_2$, 6 mM EGTA, 10 mg of aprotinin per ml, 10 mg of leupeptin per ml, and 2 mM phenylmethylsulfonyl fluoride (JS buffer). Alternatively, the cells were harvested and assayed for chloramphenicol acetyltransferase (CAT) enzymatic activity.

Western blot and immunoprecipitation analysis. Protein concentration was determined by a modification of the Bradford method (Bio-Rad). Equal amounts of proteins were separated on a reducing sodium dodecyl sulfate–7.5% polyacrylamide gel electrophoresis (SDS–7.5% PAGE) gel, transferred onto a membrane, and, subsequently, immunostained with an antibody directed against a peptide from the carboxy terminus of the RET protein (Santa Cruz Biotechnology, Heidelberg, Germany), an antiphosphotyrosine (anti-*p*-Tyr) monoclonal antibody (ICN Biochemicals, Cleveland, Ohio), or an anti-Flag monoclonal antibody (ICN Biochemicals). The long version of RET was detected with an immune serum raised against a peptide derived from the unique C terminus extension of the protein. This immune serum does not recognize the short version of the receptor or the Flag mutants. Detection was achieved by chemiluminescence with the ECL kit (Amersham, Little Chalfont, Buckinghamshire, United Kingdom). To detect RET dimers, electrophoresis was carried out with an SDS–7% PAGE gel in nonreducing conditions. Immunoprecipitation was accomplished by mixing 1 mg of protein extracts from transfected cells with anti-longRET or anti-Flag antibodies. The components of the immunocomplexes were subsequently identified by Western blotting using anti-Flag or anti-longRET antibodies, respectively.

Immunofluorescence staining. Cos cells seeded on glass coverslips were transfected with proto*RET*, *RET*2A, HSCR32, proto*RET*-Flag, and *RET*2A-Flag cDNAs. Forty-eight hours after transfection, cells were fixed with 3.7% formaldehyde for 20 min at room temperature, permeabilized with 0.1% Triton X-100 in phosphate-buffered saline for 5 min at room temperature, and processed for immunofluorescence staining. Cells were incubated with rabbit anti-RET serum or mouse anti-Flag monoclonal antibody for 20 min at room temperature, washed, and treated with donkey anti-rabbit immunoglobulin G (IgG; Texas Red linked) or with donkey anti-mouse Ig (Texas Red linked) (Amersham), respectively, for 20 min at room temperature. Pictures were taken with a 63× magnification lens.

Endo-H digestion. Equal amounts of protein extracts from proto*RET*, *RET*2A, HSCR32, proto*RET*-Flag, and *RET*2A-Flag cDNA-transfected cells were denatured at 97°C in a digestion buffer (0.2 M tribasic sodium citrate [pH 5.5], 0.5% SDS, 1 M β-mercaptoethanol, 0.5 mM phenylmethylsulfonyl fluoride). Some of the extracts were mixed with Endo-H enzyme (Boehringer GmbH, Mannheim, Germany), and all were incubated at 37°C overnight. The products were analyzed by Western blotting with an anti-RET antibody.

CAT assay. Forty-eight hours posttransfection, cells were harvested by scraping, pelleted at 13,000 × *g* for 10 min, resuspended in 100 μl of 250 mM Tris (pH 7.5), and lysed by four cycles of freezing and thawing. The extracts were cleansed of cell debris by centrifugation at 13,000 × *g* for 10 min. The CAT assay was performed with the CAT-Elisa detection kit (Boehringer GmbH) by following the manufacturer's instructions. Normalization for variations in transfection efficiency was done by quantitating the proteins with the Bio-Rad protein assay kit.

RESULTS

Analysis of RET mutants after transfection into Cos cells. To investigate the role that modifications in the outermost part of the extracellular region of RET play in its cellular localization and functional activity, two mutants were examined. One mutant carried an HSCR-associated point mutation at codon 32 that replaces a serine with a leucine residue (6). The other mutant carried an extra amino acid sequence, which enabled us to establish whether mutations different from those associated with HSCR could affect RET function. The latter mutation was generated by inserting a short DNA segment coding for an additional polyaspartic acid (Flag epitope) into the 5′ region of proto*RET* and *RET*2A cDNAs at a unique *Eag*I restriction enzyme site. These constructs were designated proto*RET*-Flag and *RET*2A-Flag, respectively. Expression vectors carrying the various cDNAs, driven either by a viral long terminal repeat (proto*RET* and the HSCR32 mutant) or by the simian virus 40 promoter-enhancer cassette (proto*RET*, *RET*2A, proto*RET*-Flag, and *RET*2A-Flag), were transiently transfected into Cos cells, which have negligible levels of endogenous RET protein. Cos cells constitute a reproducible system with which to analyze the effects of *RET* mutations (8). Protein extracts were prepared 48 h after transfection and analyzed by Western blotting using anti-RET polyclonal antibodies raised against a peptide from RET's carboxy-terminal region. Proto*RET* and *RET*2A expressed the 150- and 170-kDa species, the immature and mature forms of the protein, respectively (Fig. 1A, lane 1, and 1B, lanes 1 and 2). In contrast, only the 150-kDa partially glycosylated form of the receptor was detected in the extracts from HSCR32-, proto*RET*-Flag-, and *RET*2A-Flag-transfected cells (Fig. 1A, lane 2, and 1B, lanes 3 and 4).

Subcellular localization of the 150-kDa RET form. To determine the subcellular localization of the 150-kDa form, we

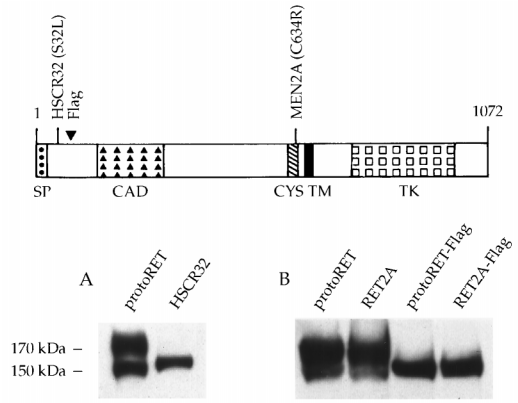

FIG. 1. Expression of *RET* mutants in Cos cells. (Top) Scheme of the short isoform of the RET protein (35). SP, signal peptide; CAD, cadherin-like domain; CYS, cysteine-rich tract; TM, transmembrane region; TK, tyrosine kinase domain; 1072, the number of amino acids in the protein. The positions of the mutants analyzed are also shown. (A and B) Cos 7 cells were transfected with 5 μg of each *RET* construct. Forty-eight hours later, cells were harvested and protein extracts were prepared. Equal amounts of proteins (100 μg) from the transfectants (indicated above the lanes) were loaded in each lane and fractionated on an SDS–7.5% PAGE gel. After transfer, the proteins were detected by using anti-RET antibodies. The migration of the mature and immature RET forms is indicated on the side.

digested the same protein extracts from transfected Cos cells with Endo-H. This enzyme digests the N-linked incomplete oligosaccharides of the proteins before they are processed to the mature carbohydrate chains in the Golgi complex. Proteins that have undergone complete glycosylation are insensitive to Endo-H, whereas partially glycosylated proteins are sensitive to its action. Equal amounts of protein extracts from proto*RET*, *RET*2A, HSCR32, proto*RET*-Flag, and *RET*2A-Flag cDNA-transfected cells were incubated with or without Endo-H, and the products were analyzed by Western blotting with anti-RET antibodies. The unique 150-kDa forms of HSCR32, protoRET-Flag, and RET2A-Flag were completely digested, and a band of about 120 kDa was detected in all samples (Fig. 2, lanes 5 to 10). Proto*RET* and *RET*2A produced the 170- and 150-kDa forms, and in both cases only the 150-kDa species was digested, resulting in the same 120-kDa band. As expected, the completely glycosylated 170-kDa form was not digested (Fig. 2, lanes 1 to 4).

We performed immunofluorescence assays to verify these results. Cos cells grown on coverslips were transfected with proto*RET*, *RET*2A, HSCR32, proto*RET*-Flag, and *RET*2A-Flag expression vectors, fixed with formaldehyde, permeabilized with Triton X-100, and stained with anti-RET antibodies.

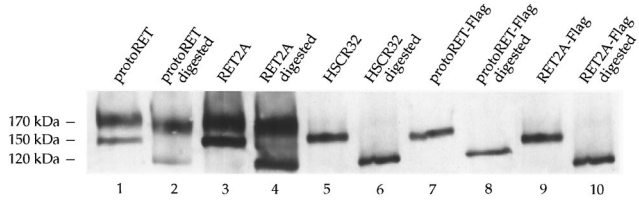

FIG. 2. Endo-H sensitivities of the different RET forms. Cos cells were transfected with the *RET* constructs indicated above the lanes and harvested 48 h later. Protein extracts were prepared and treated with Endo-H or were left untreated. The products were analyzed on an SDS–7.5% PAGE gel and immunostained with anti-RET antibodies. The migration of the fully glycosylated and partially glycosylated proteins and of the digestion product is shown on the left.

The proto*RET*-Flag- and *RET*2A-Flag-transfected cells were stained also with anti-Flag-specific monoclonal antibodies. The positive immunofluorescence signal detectable in cells transfected with proto*RET* and *RET*2A was distributed in the rough endoplasmic reticulum through the Golgi complex to the plasma membrane (Fig. 3A and B). In cells transfected with HSCR32, proto*RET*-Flag, and *RET*2A-Flag there was a positive perinuclear staining, particularly evident around the nuclear membrane, suggesting a localization in the endoplasmic reticulum (Fig. 3C, D, and E). The same pattern was obtained with anti-Flag antibodies (Fig. 3F and G). No staining was observed with either antibody in mock-transfected or nonpermeabilized cells (data not shown).

The 150-kDa RET species can form homodimers. To characterize the biochemical properties of the 150-kDa RET species, protein extracts from proto*RET*, *RET*2A, HSCR32, proto*RET*-Flag, and *RET*2A-Flag cDNA-transfected cells were fractionated on nonreducing SDS–7% PAGE gel. Equal amounts of proteins were loaded on twin gels, transferred onto a membrane, and immunoblotted with anti-RET polyclonal antibodies or anti-Flag monoclonal antibodies. As expected, a band of about 340 kDa was clearly detectable in the extracts from *RET*2A-transfected cells, due to the disulfide-bonded 170-kDa species (Fig. 4A, lane 2). A band of approximately 300 kDa was barely visible in extracts from cells transfected with proto*RET* and was more intense with HSCR32, proto*RET*-Flag, and *RET*2A-Flag (Fig. 4A, lanes 1, 3, 4, and 5). Since the 150-kDa species is the only species produced by the last three constructs, the band detected can only result from the dimerization of this form. Similar results were obtained with proto*RET*-Flag and *RET*2A-Flag extracts by using the anti-Flag antibody (Fig. 4B, lanes 1 and 2). In addition to the dimer bands, bands corresponding to the monomeric forms of RET were detected in the lanes corresponding to protoRET, HSCR32, and protoRET-Flag (Fig. 4A, lanes 1, 3, and 4, and 4B, lane 1) and were barely visible, if at all, in lanes corresponding to RET2A and RET2A-Flag (Fig. 4A, lanes 2 and 5, and 4B, lane 2). These forms appeared slightly smudged because of the long gel run. Finally, very large protein complexes or aggregates were stained by both anti-RET and anti-Flag antibodies (Fig. 4). The possibility that GDNF receptor α could participate in these complexes was excluded, as it is not expressed in Cos cells, as proved by reverse transcription-PCR (data not shown).

Phosphorylation of the RET mutants. Phosphorylation on tyrosine residues in vivo was then examined to evaluate the kinase activities of HSCR32, protoRET-Flag, and RET2A-Flag compared to those of protoRET and RET2A. Equal amounts of proteins from transfected cells were loaded on twin gels and immunoblotted with anti-RET antibodies or an anti-*p*-Tyr monoclonal antibody. Although all different RET proteins were expressed at high and comparable levels (Fig. 5A, lanes 1 to 5), a variable phosphorylation was detected. HSCR32 and protoRET-Flag displayed phosphorylation levels that were lower than the basal one associated with protoRET (Fig. 5B, lanes 1, 3, and 4); RET2A-Flag was much less phosphorylated than the activated RET2A (Fig. 5B, lanes 2 and 5).

Transactivation potentials of the *RET* mutants. The various *RET* constructs were tested for their abilities to transactivate a reporter plasmid in transient cotransfection assays. The TRE-TK-CAT plasmid, in which the TK-CAT gene was fused to a tetradecanoyl phorbol acetate-responsive element oligonucleotide (TRE), was used as the target gene. The TRE is the binding site for the AP1 complex and is derived from the collagenase promoter region. Following the binding of RET with the cognate ligand, the Ras-Raf mitogen-activated protein

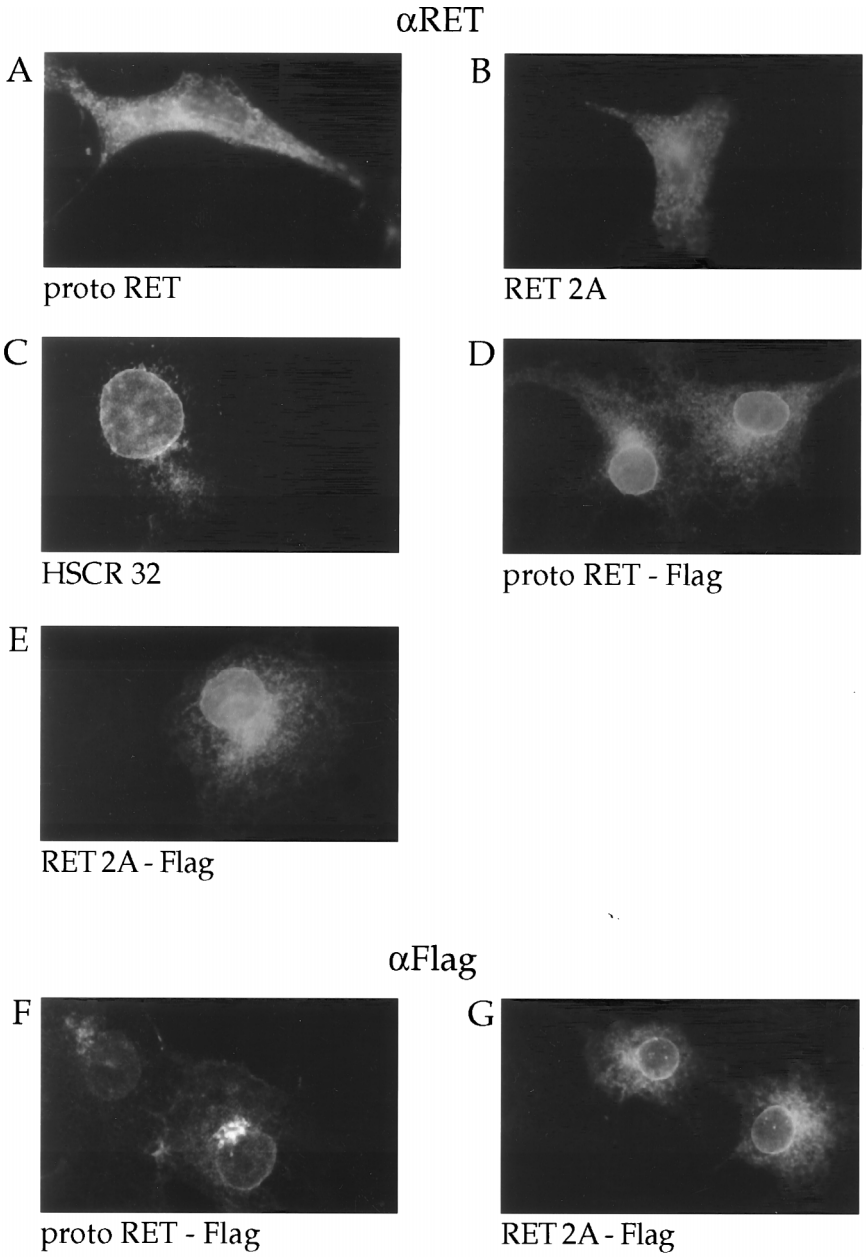

FIG. 3. Immunofluorescence analysis of the RET mutants. Cos cells grown on coverslips were transfected with the various *RET* constructs as indicated. They were then fixed, permeabilized, and stained with anti-RET (αRET) (A to E) or anti-Flag (αFlag) (F and G) antibodies.

kinases constitute, in fact, the major intracellular signalling pathway activated (40). This cascade of events leads to the formation of Jun-Fos dimers and binding to responsive elements of the target genes. A constant amount of the reporter plasmid was cotransfected with different ratios (1:1, 1:2, and 1:3) of the various *RET* mutants. A dose-response curve that was repeatedly observed with different DNA preparations and in at least three independent experiments was obtained (Fig. 6). The empty vectors alone showed no activity; proto*RET* caused a basal level of induction, while *RET*2A induced a level of CAT activity about fourfold higher than that induced by proto*RET*. The HSCR32 mutant and the Flag-containing constructs did not transactivate the reporter plasmid. The HSCR32 data confirmed in our system the findings obtained with PC12 cells (6).

Dominant negative effect of the *RET* mutants. To establish whether HSCR32 and the Flag mutants exert a dominant negative effect, we performed transient cotransfections with a fixed amount of proto*RET* and three molar ratios of the various mutants (1:1, 1:2, and 1:3). proto*RET* and HSCR32 mutant plasmids, individually transfected, produced the 170- and 150-kDa bands and the 150-kDa band, respectively (Fig. 7A, lanes 1 and 2). When proto*RET* and HSCR32 were cotransfected, the mature 170-kDa form was detected at low levels at the 1:1 ratio and completely disappeared with the increase of the cotransfected mutant plasmid (Fig. 7A, lanes 3 to 5). The 150-

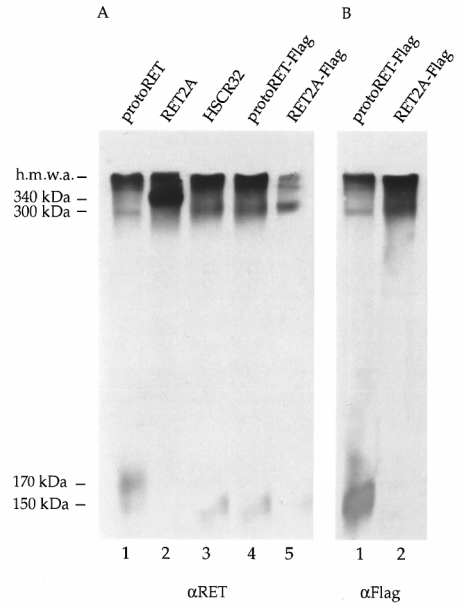

FIG. 4. Dimer formation of the different RET mutants. (A) Equal amounts of proteins from Cos cells transfected with the proto*RET*, *RET*2A, HSCR32, proto*RET*-Flag, and *RET*2A-Flag constructs were fractionated on nonreducing SDS–7% polyacrylamide gel, transferred, and stained with anti-RET (αRET) antibodies. (B) Equivalent protein extracts from cells transfected with proto*RET*-Flag and *RET*2A-Flag constructs were processed similarly and stained with anti-Flag (αFlag) antibodies. The migration of the monomers, dimers, and high-molecular-mass aggregates (h.m.w.a.) is indicated on the left. The sizes of the dimers were determined on the basis of the migration of size markers of known molecular weights.

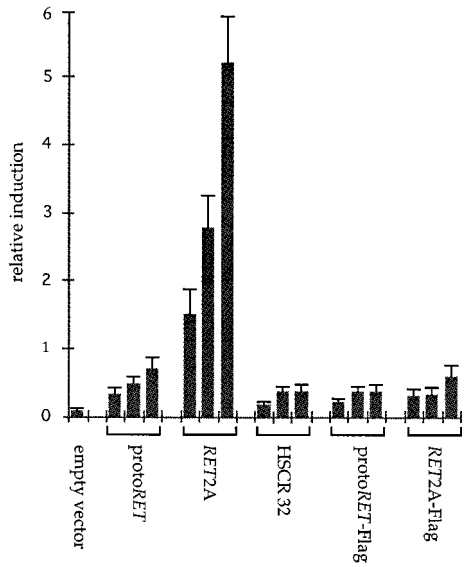

FIG. 6. Transactivation abilities of *RET* mutants. Cos cells were transfected with a constant amount (5 μg) of the TRE-TK-CAT reporter gene and three different molar ratios (from left to right, for each expression vector, 1:1, 1:2, and 1:3) of each of the expression vectors for proto*RET*, *RET*2A, HSCR32, proto*RET*-Flag, and *RET*2A-Flag. Each CAT activity is reported as relative induction and represents the mean of at least three independent experiments performed with different DNA preparations. Standard deviations are indicated by error bars.

kDa band, on the other hand, markedly increased. Transfections with proto*RET* and proto*RET*-Flag plasmids, carried out under the same experimental conditions, produced similar results. In this case also, cotransfections of the mutant plasmid caused a drastic reduction of the 170-kDa form even at the 1:1 ratio and complete abrogation at higher proportions (Fig. 7B, lanes 1 to 5). Cotransfection of proto*RET* with increasing amounts of an empty vector did not affect the accumulation of the 170-kDa form, excluding promoter competition effects. In contrast, the amount of the mature form increased proportionally with the amount of proteins loaded in each lane (Fig. 7, panel C).

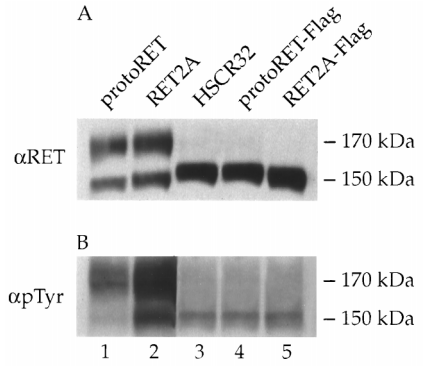

FIG. 5. Expression and tyrosine phosphorylation of RET mutants. Equivalent amounts of protein extracts from cells transfected with the various constructs were analyzed by Western blotting for the expression levels of the various forms of RET with anti-RET (αRET) antibodies (A). The same amounts of proteins were analyzed for tyrosine phosphorylation with an anti-*p*-Tyr (αpTyr) antibody (B). The migration of the 170- and 150-kDa RET monomers is indicated at the right of both panels.

The same extracts were analyzed for the maturation of an endogenous protein to control the glycosylation process. The β subunit of the membrane-bound ATPase is a membrane protein only in its fully glycosylated form. This 55-kDa protein was detected as a single band of the expected size in all extracts analyzed, ruling out the possibility that the glycosylation machinery was saturated or slowed down by overproduction of the transfected proteins (data not shown). To confirm that the data obtained were not due to an overload of the cells with exogenous proteins but rather to a specific heterodimerization event, the converse experiment was performed. Constant amounts of HSCR32 or proto*RET*-Flag were cotransfected with increasing ratios of proto*RET*. A proportional increase of the 170-kDa band occurred in the lanes corresponding to the cotransfectants, together with an increase of the 150-kDa band (Fig. 7D and E, lanes 1 to 5). This effect was specific because cotransfection of an empty vector or a plasmid expressing an unrelated protein did not produce the 170-kDa band (Fig. 7D and E, lanes 6 and 7). We also demonstrated that the formation of the RET2A 170-kDa form was impeded in cotransfections with increasing amounts of the *RET2A*-Flag mutant expression vector, as shown for proto*RET* (Fig. 8A, lanes 1 to 5).

To correlate the maturation block with the biological activities of the various RET forms, we performed transactivation-cotransfection experiments. The TRE-TK-CAT and the *RET*2A plasmids were used as the target and transactivating vectors, respectively. The *RET*2A construct was the only one able to transactivate a reporter gene and was used at the 1:3 ratio shown before to produce the highest level of induction (Fig. 6). The addition of *RET*2A-Flag vector to the cotransfection mixture at 1:1, 1:2, and 1:3 ratios, with respect to the *RET*2A vector, nearly abolished the CAT activity of the target gene (Fig. 8B). Similar results were obtained with HSCR32

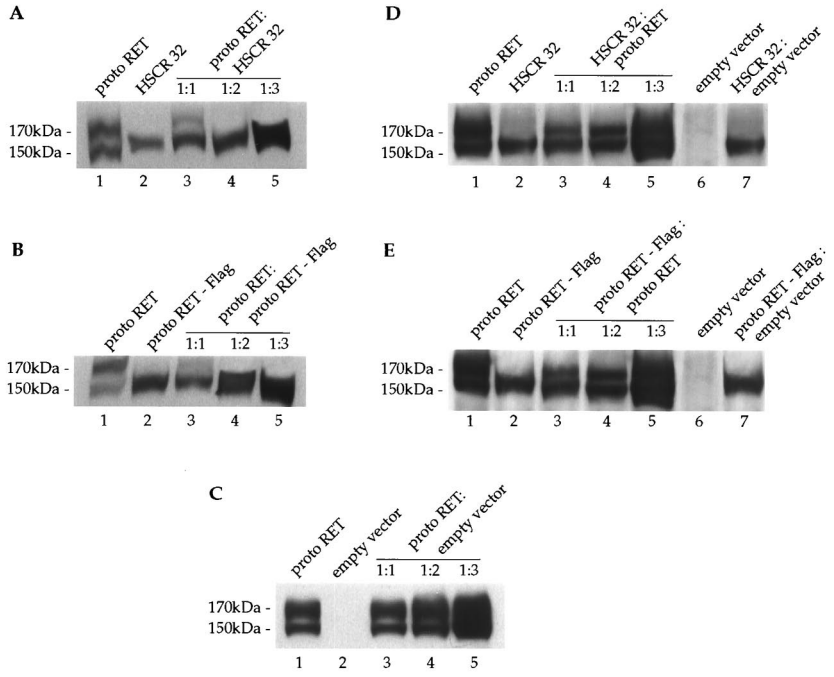

FIG. 7. HSCR32 and proto*RET*-Flag mutants exert a dominant negative effect over proto*RET*. (A) Cos cells were cotransfected with 5 μg of proto*RET* and 5, 10, and 15 μg of proto*RET*-Flag expression vectors. Parallel transfections were carried out with 5 μg of proto*RET* and proto*RET*-Flag expression vectors alone. A Western blot analysis was performed with increasing amounts of proteins from the transfected cells. Lane 1, protoRET (50 μg); lane 2, HSCR32 (50 μg); lanes 3 to 5, protoRET and HSCR32 at ratios of 1:1 (100 μg) (lane 3), 1:2 (150 μg) (lane 4), and 1:3 (200 μg) (lane 5). After the immunoblotting, the RET species were stained with anti-RET antibodies. The migration of the 170- and 150-kDa RET monomers is indicated. (B) Western blot analysis performed as described for panel A on different amounts of protein extracts from cells individually transfected with proto*RET* and proto*RET*-Flag expression plasmids (lanes 1 and 2) or cotransfected at three molar ratios (lanes 3 to 5). The migration of the 170- and 150-kDa RET monomers is indicated. (C) Western blot analysis performed on protein extracts from cells individually transfected with proto*RET* or an empty vector (lanes 1 and 2) or cotransfected in three molar ratios (lanes 3 to 5). The RET species were identified by immunoblotting with anti-RET antibodies. (D) Western blot analysis performed as described for panel A on different amounts of proteins from cells transfected with proto*RET* and HSCR32 alone (lanes 1 and 2) or with a combination of a fixed amount of HSCR32 and three ratios of proto*RET* expression vector (lanes 3 to 5). In lanes 6 and 7 extracts from cells transfected with an empty vector alone or cotransfected with HSCR32 and an empty vector at a 1:3 ratio are shown. The RET species were identified with anti-RET antibodies. (E) Western blot analysis of protein extracts from cells transfected with proto*RET* and proto*RET*-Flag expression vectors alone (lanes 1 and 2) or cotransfected with a fixed amount of proto*RET*-Flag and three proportions of proto*RET* (lanes 3 to 5). Extracts from cells transfected with an empty vector or with proto*RET*-Flag and an empty vector at a 1:3 ratio were loaded in lanes 6 and 7. The RET species were identified with anti-RET antibodies.

(Fig. 8C) and proto*RET*-Flag (data not shown) expression vectors. Taken together these results demonstrate a clear correlation between the lack of production of the 170-kDa form and the loss of RET biological function.

Finally, to demonstrate that both the wild-type and mutant RET forms were expressed during the course of the experiments, we transfected Cos cells with plasmids expressing proteins that could differentially be identified by specific antibodies. This strategy allows the determination of the type and the amount of each protein synthesized from the transfected cDNAs. The proto*RET*-Flag expression vector was cotransfected in three increasing molar ratios (1:1, 1:2, and 1:3) with a constant amount of a plasmid expressing long*RET*. This protein contains an additional stretch of 51 aa at its C terminus (13) and is recognized by a specific antiserum that does not identify either protoRET or protoRET-Flag. Long*RET* and the Flag mutant cDNAs were also transfected alone, as controls (Fig. 9A and B, lanes 1 and 2). Protein extracts from the transfected cells were loaded as described above on twin gels, fractionated by SDS-PAGE, transferred, and immunostained with anti-longRET or anti-Flag antibodies. The anti-RET antibodies recognized both longRET species: the 170-kDa form was already diminished at the 1:1 ratio and completely disappeared at the 1:2 and 1:3 ratios (Fig. 9A, lanes 3 to 5); the 150-kDa form was present and increased in the extracts at the 1:2 and 1:3 ratios. The anti-Flag antibodies recognized only the 150-kDa form produced by the Flag mutant, which increased with the amount of the proteins loaded (Fig. 9B, lanes 3 to 5; see also the experiments described above). Similar results were obtained in cotransfections of long*RET* cDNA with HSCR32 and *RET*2A-Flag expression vectors (data not shown).

To investigate whether longRET and the Flag mutant were capable of interacting and forming heterodimers, protein extracts from cotransfected Cos cells were immunoprecipitated with anti-longRET or anti-Flag antibodies. The complexes were subsequently immunoblotted with anti-Flag or anti-longRET antibodies, respectively. In the anti-longRET immunoprecipitates derived from cotransfected Cos cells, the immunoblot with the same antibodies identified a single band of 150 kDa (Fig. 9C, lane 5). A similar band was recognized by the anti-Flag antibodies (lane 6). In contrast, when the extracts from cells transfected with the long*RET* construct alone were immunoprecipitated and immunostained with the same antibodies, both 170- and 150-kDa longRET forms were recognized (lane 1). The anti-Flag antibodies did not recognize any band in these immunocomplexes (lane 2). In the reverse experiment, when the extracts derived from the same cotransfected cells were immunoprecipitated and immunoblotted with the anti-Flag antibodies, a single band of 150-kDa was detected; immunoblotting with the anti-longRET antibodies revealed also a 150-kDa band (lanes 7 and 8). Protein extracts from the protoRET-Flag single transfectant immunoprecipitated and

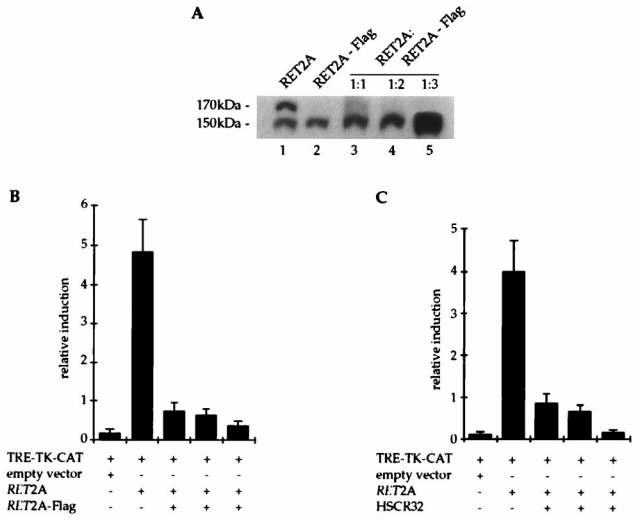

FIG. 8. *RET*2A-Flag mutant exerts a dominant negative effect over an activated *RET*2A. (A) Western blot analysis of equivalent protein extracts from cells transfected with the *RET*2A and *RET*2A-Flag expression vectors alone (lanes 1 and 2) or together at three different molar ratios (lanes 3 to 5). The RET forms were stained with anti-RET antibodies. The migration of the 170- and 150-kDa RET monomers is indicated. (B and C) Transactivation-cotransfection assay performed with the TRE-TK-CAT plasmid (2 μg) as the reporter, the *RET*2A carrying vector as the transactivator at a 1:3 ratio (6 μg), and the *RET*2A-Flag (B)- or HSCR32 (C)-containing plasmid in three molar ratios with respect to *RET*2A plasmid (6, 12, and 18 μg). An empty vector was used as the negative control of the experiments. CAT activity is reported as relative induction and represents the mean of at least three independent experiments performed with different DNA preparations. The standard deviation is indicated by error bars. +, species is present; −, species is absent.

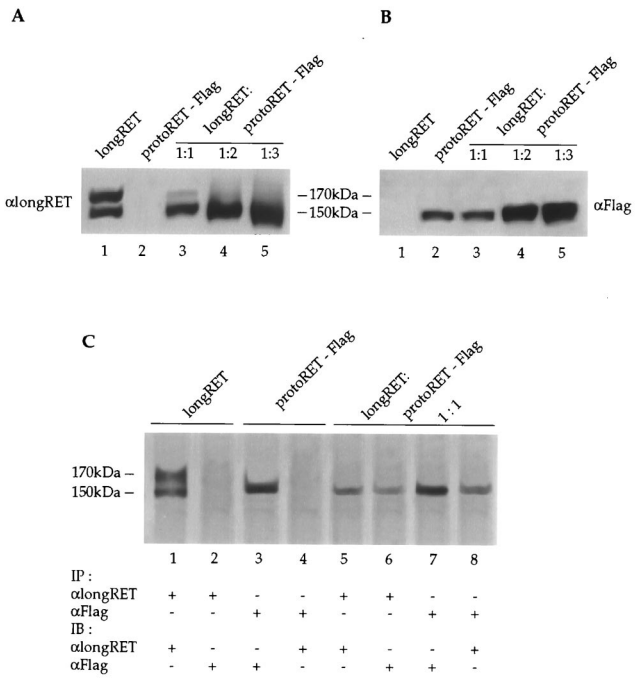

FIG. 9. LongRET and the Flag mutant are coexpressed and form heterodimers in cotransfected cells. (A and B) Cos cells were cotransfected with 5 μg of long*RET* and 5, 10, and 15 μg of proto*RET*-Flag expression vectors. Parallel transfections were carried out with 5 μg of long*RET* and proto*RET*-Flag expression vectors alone. A Western blot analysis was performed with increasing amounts of proteins from the transfected cells. Lane 1, longRET (50 μg); lane 2, protoRET-Flag (50 μg); lanes 3 to 5, protoRET and protoRET-Flag at a 1:1 ratio (100 μg) (lane 3), at a 1:2 ratio (150 μg) (lane 4), and at a 1:3 ratio (200 μg) (lane 5). After the immunoblotting, the RET species were stained with either anti-longRET- or anti-Flag-specific antibodies, as indicated. The migration of the 170- and 150-kDa RET monomers is shown. (C) Immunoprecipitation and immunoblotting experiments. One milligram of protein extracts from Cos cells transfected with long*RET* and proto*RET*-Flag expression vectors alone or cotransfected at a 1:1 molar ratio was subjected to immunoprecipitation with anti-longRET (αlongRET) (lanes 1, 2, 5, and 6) or anti-Flag (αFlag) antibodies (lanes 3, 4, 7, and 8). The anti-longRET immunocomplexes were subsequently stained with the same antibodies (lanes 1 and 5) or with the anti-Flag antibodies (lanes 2 and 6). The anti-Flag immunoprecipitates were stained with the same antibodies (lanes 3 and 7) or with anti-longRET antibodies (lanes 4 and 8). The migration of the 170- and 150-kDa RET monomers is shown.

immunoblotted with the anti-Flag antibodies recognized only the 150-kDa species (lane 3); no bands were recognized by the anti-longRET antibodies on the same immunocomplexes (lane 4). These results demonstrate that the 150-kDa mutant form is capable of heterodimerizing with the 150-kDa wild-type species.

DISCUSSION

Role of the extracellular region in the maturation of the RET receptor. We investigated the effects of two mutations located at the extreme N terminus of the extracellular region of the product of the *RET* proto-oncogene on the biochemical and biological activity of the whole receptor. The HSCR32 mutation affects an amino acid residue which is highly conserved among species and is associated with a long form of HSCR (6, 17). In this respect, HSCR32 is similar to all other mutants associated with this disease. We asked whether mutants carrying an insertion at the N-terminal part, such as the Flag-containing mutant analyzed here, could have similar effects. The two mutants behaved similarly: they inhibited the production of the mature 170-kDa form and its exposure on the cell membrane by interfering with the glycosylation process. The immature 150-kDa form accumulated in the endoplasmic reticulum, as shown also by immunofluorescence studies and by the sensitivity of this form to Endo-H digestion. Other HSCR mutants with mutations in the extracellular domain (6, 17) and at the putative calcium binding site of the cadherin-like domain interfered with RET maturation (2). From these data it appears that the correct folding of the extracellular region plays a crucial role in the maturation, in the intracellular transport, and, ultimately, in the function of RET. This region, with the exclusion of the cysteine-rich tract, behaves as an independent structural and functional domain, because the maturation block was detected also with the double mutant *RET*2A-Flag, a *RET* mutant with a MEN 2A mutation.

The 150-kDa species can form homodimers. The results of this study show that the 150-kDa RET form was able to form dimers before its insertion into the plasma membrane and in the absence of the ligand. Therefore, accumulation of the protein in the endoplasmic reticulum seems to facilitate dimerization, and the larger the amount of protein retained, the greater the number of dimers formed. In fact, dimers were barely detectable in protoRET, were abundant in protoRET-Flag, and were more abundant in RET2A-Flag. This increase is probably a result of their higher degree of stability brought about by the covalent bonds generated by the mispaired cysteine residues. As a consequence, the monomeric forms, practically undetectable in the *RET*2A constructs, were still evident in the proto*RET* plasmid. The data suggest that the processing of the receptor may involve a dimerization step of the 150-kDa form. We also detected high-molecular-weight aggregates, the

biological significance of which is not yet clear. More experiments are required to elucidate their origin and composition. They were, in fact, resistant to heat and to denaturing conditions; disulfide bonds and noncovalent interactions may be responsible for their formation, and other proteins may participate in these complexes.

Intracellular dimerization has been reported for the products of other activated oncogenes and is due to protein domains artificially fused after translocation or genomic rearrangements. *RET*/PTCII codes for a protein in which the RET tyrosine kinase domain is fused to the N terminus from the R1α regulatory subunit of the protein kinase A that provides the structural motifs for intracellular dimerization (4). Also, the *Trk* gene is activated in several tumors via a mechanism of gene rearrangement, in which its kinase domain becomes juxtaposed to heterologous sequences, such that the resulting protein can form intracellular homodimers (9). A structurally altered form of the *Ron* gene product is not exposed on the cell surface; the products are retained intracellularly as dimers and oligomers stabilized by intermolecular disulfide bonds (7). Finally, an intragenic deletion of the *Met* oncogene leads to the formation of a mutant protein that has an uneven number of cysteine residues in the extracellular domain and that is altered in its folding and blocked in its maturation (27). In all these cases, the mutant proteins display constitutive tyrosine phosphorylation and cause the expressing cells to become transformed. The mutations of the *RET* proto-oncogene described in this report behave differently.

Phosphorylation, transactivation potentials, and biological effects of the mutants analyzed. The mutations analyzed in this study hampered the kinase activity of the receptor. HSCR32 and the Flag mutants showed low-level, if any, tyrosine phosphorylation compared with the basal level of phosphorylation of protoRET and with the high level of phosphorylation of RET2A. This low level of phosphorylation activity was associated with a lack of the transactivation potential and therefore with a lack of function. *RET*2A, in fact, induced CAT activity, while proto*RET* caused only a slight increase; HSCR32, proto*RET*-Flag, and *RET*2A-Flag showed no significant induction. The low level of phosphorylation activity of the HSCR32 and Flag constructs may be attributed to inter- and intramolecular phosphorylation of the 150-kDa species accumulated as dimers in the endoplasmic reticulum. The 150-kDa dimers, however, were not active in transactivation (Fig. 6). The low levels of phosphorylation and transactivation potential associated with protoRET could, instead, be ascribed to the mature 170-kDa species and to its low level of intrinsic kinase activity (37).

The cotransfection experiments demonstrated that the *RET* mutants interfere with the formation of the 170-kDa species derived from the cotransfected proto*RET* and *RET*2A plasmids. This effect was very intense at a ratio of 1:1, suggesting that, already in this condition, the mutant RET impairs the synthesis of the mature 170-kDa species from the wild-type allele and its exposure on the membrane. At higher proportions of the mutant plasmids, the mature 170-kDa form completely disappeared. As shown by the reverse experiments and by the controls, the effects observed were specifically due to the mutant RET species produced over the wild-type form. The cotransfection and immunoprecipitation experiments with the long*RET* expression vector demonstrated that the mutant RET species were expressed together with the wild-type forms and were capable of interacting and forming a heteromeric complex with the corresponding 150-kDa form from the normal allele. The transactivation-cotransfection experiments finally demonstrated that the heteromeric complexes did not transactivate a target gene: *RET*2A CAT activity was diminished to complete abrogation in the presence of increasing amounts of the mutants. The maturation block thus correlates with the reduction and abolition of the biological function of the RET receptor.

On the basis of the data reported in this manuscript, we propose a molecular mechanism to explain the pathogenesis of the HSCR disease cases due to mutations in the extracellular region of RET. The 150-kDa mutant form accumulates in the endoplasmic reticulum and heterodimerizes with the RET precursors derived from the normal allele. These are "sequestered" by the mutant forms and are impeded from maturing fully and from being inserted into the cell membrane. The mutant HSCR forms, then, act as dominant negative forms overwhelming the wild-type RET protein and preventing it from functioning. This effect is very evident at a 1:1 ratio, a condition similar to the heterozygous state of HSCR disease patients, suggesting that an active RET receptor is critical for the full development of the enteric ganglia in humans. The mechanism proposed here for HSCR mutations in the extracellular region of RET parallels the one proposed for intracytoplasmic HSCR mutations (8, 25). In conclusion, all HSCR disease cases in which RET is involved are caused by mutations scattered throughout the associated gene that result in a clinical picture typical of loss of function of the receptor by a mechanism of negative dominance.

ACKNOWLEDGMENTS

This work was supported by grants from the CNR, Progetto Finalizzato ACRO, Sottoprogetto 4, and from Associazione Italiana per la Ricerca sul Cancro (AIRC).

We thank V. E. Avvedimento, S. Bonatti, and M. Grieco for suggestions and critical reading of the manuscript. We thank J. Gilder for editing the text. The technical assistance of Maurizio Lamagna is gratefully acknowledged.

REFERENCES

1. **Angrist, M., S. Bolk, B. Thiel, E. G. Puffemberger, R. M. W. Hofstra, C. H. C. M. Buys, D. T. Cass, and A. Chakravarti.** 1995. Mutation analysis of the RET receptor tyrosine kinase in Hirschsprung disease. Hum. Mol. Genet. **4:**821–830.
2. **Asai, N., T. Iwashita, M. Matsuyama, and M. Takahashi.** 1995. Mechanism of activation of the *ret* proto-oncogene by multiple endocrine neoplasia 2A mutations. Mol. Cell. Biol. **15:**1613–1619.
3. **Avantaggiato, V., N. A. Dathan, M. Grieco, N. Fabien, D. Lazzaro, A. Fusco, A. Simeone, and M. Santoro.** 1994. Developmental expression of the *RET* proto-oncogene. Cell Growth Differ. **5:**305–311.
4. **Bongarzone, I., N. Monzini, M. G. Borrello, C. Carcano, G. Ferraresi, E. Arighi, P. Mondellini, G. Della Porta, and M. A. Pierotti.** 1993. Molecular characterization of a thyroid tumor-specific transforming sequence formed by the fusion of *ret* tyrosine kinase and the regulatory subunit RIα of cyclic AMP-dependent protein kinase A. Mol. Cell. Biol. **13:**358–366.
5. **Buj Bello, A., J. Adu, L. G. Pinon, A. Horton, J. Thompson, A. Rosenthal, M. Chinchetru, V. L. Buchman, and A. M. Davies.** 1997. Neurturin responsiveness requires a GPI-linked receptor and the Ret receptor tyrosine kinase. Nature **387:**721–724.
6. **Carlomagno, F., G. De Vita, M. T. Berlingieri, V. de Franciscis, R. M. Melillo, V. Colantuoni, M. H. Kraus, P. P. Di Fiore, A. Fusco, and M. Santoro.** 1996. Molecular heterogeneity of RET loss of function in Hirschsprung's disease. EMBO J. **15:**2717–2725.
7. **Collesi, C., M. Santoro, G. Gaudino, and P. Comoglio.** 1996. A splicing variant of the RON transcript induces contitutive tyrosine kinase activity and an invasive phenotype. Mol. Cell. Biol. **16:**5518–5526.
8. **Cosma, M. P., L. Panariello, L. Quadro, N. A. Datan, O. Fattoruso, and V. Colantuoni.** 1996. A mutation in the *RET* proto-oncogene in Hirschsprung's disease affects the tyrosine kinase activity associated with multiple endocrine neoplasia type 2A and 2B. Biochem. J. **314:**397–400.
9. **Coulier, F., R. Kumar, M. Ernst, R. Klein, D. Martin-Zanca, and M. Barbacid.** 1990. Human *trk* oncogenes activated by point mutation, in-frame deletion, and duplication of the tyrosine kinase domain. Mol. Cell. Biol. **10:**4202–4210.
10. **Donis-Keller, H., S. Dou, D. Chi, K. M. Carlson, K. Toshima, T. C. Lairmore, J. R. Howe, P. Goodfellow, and S. A. Wells.** 1993. Mutations in the *RET* proto-oncogene are associated with MEN2A and FMTC. Hum. Mol. Genet. **2:**851–856.

11. **Durbec, P., C. V. Marcos Gutierrez, C. Kilkenny, M. Grigoriou, K. Wartiowaara, P. Suvanto, D. Smith, B. Ponder, F. Costantini, M. Saarma, H. Sariola, and V. Pachnis.** 1996. GDNF signalling through the Ret receptor tyrosine kinase. Nature **381:**789–793.
12. **Edery, P., S. Lyonnet, L. M. Mulligan, A. Pelet, E. Dow, L. Abel, S. Holder, C. Nihoul, B. A. J. Ponder, and A. Munnich.** 1994. Mutations of the *RET* proto-oncogene in Hirschsprung's disease. Nature **367:**378–380.
13. **Eng, C., and L. M. Mulligan.** 1997. Mutations of the RET proto-oncogene in the multiple endocrine neoplasia type 2 syndromes, related sporadic tumours, and Hirschsprung disease. Hum. Mutat. **9:**97–109.
14. **Graham, F. L., and A. J. van der Eb.** 1973. A new technique for the assay of infectivity of human adenovirus 5 DNA. Virology **52:**456–467.
15. **Hofstra, R. M. W., R. M. Landsvater, I. Ceccherini, R. P. Stulp, T. Stelwagen, Y. Luo, B. Pasini, J. W. M. Hoppener, H. K. Ploos van Amstel, G. Romeo, C. J. M. Lips, and C. H. C. M. Buys.** 1994. A mutation in the *RET* protooncogene associated with multiple endocrine neoplasia type 2B and sporadic medullary thyroid carcinoma. Nature **367:**375–376.
16. **Ikeda, I., Y. Ishizaka, T. Tahira, T. Suzuki, M. Onda, T. Sugimura, and M. Nagao.** 1990. Specific expression of the *RET* proto-oncogene in human neuroblastoma cell lines. Oncogene **5:**1291–1296.
17. **Iwashita, T., H. Murakami, N. Asai, and M. Takahashi.** 1996. Mechanism of Ret dysfunction by Hirschsprung mutations affecting its extracellular domain. Hum. Mol. Genet. **5:**1577–1580.
18. **Jing, S., D. Wen, Y. Yu, P. L. Holst, Y. Luo, M. Fang, R. Tamir, L. Antonio, Z. Hu, R. Cupples, J. C. Louis, S. Hu, B. W. Altrock, and G. M. Fox.** 1996. GDNF-induced activation of the ret protein tyrosine kinase is mediated by GDNFR-alpha, a novel receptor for GDNF. Cell **85:**1113–1124.
19. **Klein, R. D., D. Sherman, W. H. Ho, D. Stone, G. L. Bennett, B. Moffat, R. Vandlen, L. Simmons, Q. Gu, J. A. Hongo, B. Devaux, K. Poulsen, M. Armanini, C. Nozaki, N. Asai, A. Goddard, H. Phillips, C. E. Henderson, M. Takahashi, and A. Rosenthal.** 1997. A GPI-linked protein that interacts with Ret to form a candidate neurturin receptor. Nature **387:**717–721.
20. **Luo, Y., I. Ceccherini, B. Pasini, I. Matera, M. P. Bicocchi, V. Barone, R. Bocciardi, H. Kaariaiainen, D. Weber, M. Devoto, and G. Romeo.** 1993. Close linkage with the RET proto-oncogene and boundaries of deletion mutants in autosomal dominant Hischsprung disease. Hum. Mol. Genet. **11:**1803–1808.
21. **Martucciello, G., M. P. Bicocchi, P. Dodero, M. Lerone, M. S. Cirillo, A. Puliti, G. Gimelli, G. Romeo, and V. Jasonni.** 1992. Total colonic aganglionosis associated with interstitial deletion of the long arm of chromosome 10. Pediatr. Surg. Int. **7:**308–310.
22. **Mulligan, L. M., J. B. Kwok, C. S. Healey, M. J. Elsdon, C. Eng, E. Gardner, D. R. Love, S. E. Mole, and J. K. Moore.** 1993. Germline mutations of the *RET* protooncogene in multiple endocrine neoplasia type 2A families. Nature **363:**458–460.
23. **Nakamura, T., Y. Ishizaka, M. Nagao, M. Hara, and T. Ishikawa.** 1994. Expression of the ret proto-oncogene product in human normal and neoplastic tissues of neural crest origin. J. Pathol. **172:**255–260.
24. **Pachnis, V., B. Mankoo, and F. Costantini.** 1993. Expression of the c-ret proto-oncogene during mouse embryogenesis. Development **119:**1005–1017.
25. **Pasini, B., M. G. Borrello, A. Greco, I. Bongarzone, Y. Luo, P. Mondellini, L. Alberti, C. Miranda, E. Arighi, R. Bocciardi, M. Seri, V. Barone, M. T. Radice, G. Romeo, and M. A. Pierotti.** 1995. Loss of function effect of *RET* mutations causing Hirschsprung disease. Nat. Genet. **10:**35–40.
26. **Passarge, E.** 1967. The genetics of Hirschsprung's disease. N. Engl. J. Med. **276:**138–141.
27. **Rodriguez, G. A., M. A. Naujokas, and M. Park.** 1991. Alternative splicing generates isoforms of the *met* receptor tyrosine kinase which undergo differential processing. Mol. Cell. Biol. **11:**2962–2970.
28. **Romeo, G., P. Ronchetto, Y. Luo, V. Barone, M. Seri, I. Ceccherini, B. Pasini, R. Bocciardi, M. Lerone, H. Kaariainen, and G. Martucciello.** 1994. Point mutations affecting the tyrosine kinase domain of the *RET* proto-oncogene in Hirschsprung's disease. Nature **367:**377–378.
29. **Sanchez, M. P., I. Silos Santiago, J. Frisen, B. He, S. A. Lira, and M. Barbacid.** 1996. Renal agenesis and the absence of enteric neurons in mice lacking GDNF. Nature **382:**70–73.
30. **Santoro, M., R. Rosati, M. Grieco, M. T. Berlingieri, L. C. D'Amato, V. De Franciscis, and A. Fusco.** 1990. The *RET* proto-oncogene is consistently expressed in human pheochromocytomas and thyroid medullary carcinomas. Oncogene **5:**1595–1598.
31. **Santoro, M., F. Carlomagno, A. Romano, D. P. Bottaro, N. A. Dathan, M. Grieco, A. Fusco, G. Vecchio, B. Matoskova, M. H. Kraus, and P. P. Di Fiore.** 1995. Germ-line mutations of MEN2A and MEN2B activate *RET* as a dominant transforming gene by different molecular mechanisms. Science **267:**381–383.
32. **Schimke, R. N.** 1984. Genetic aspects of multiple endocrine neoplasia. Annu. Rev. Med. **35:**25–31.
33. **Schuchardt, A., V. D'Agati, L. L. Blomberg, F. Costantini, and V. Pachnis.** 1994. The c-*ret* receptor tyrosine kinase gene is required for the development of the kidney and enteric nervous system. Nature **367:**380–383.
34. **Songyang, Z., K. L. Carraway III, M. J. Eck, S. C. Harrison, R. Feldman, M. Mohammadi, J. Schlessinger, S. R. Hubbard, D. P. Smith, C. Eng, M. J. Lorenzo, B. A. J. Ponder, B. J. Mayer, and L. C. Cantley.** 1995. Catalytic specificity of protein-tyrosine kinases is critical for selective signalling. Nature **373:**536–539.
35. **Takahashi, M., Y. Buma, T. Iwamoto, Y. Inaguma, H. Ikeda, and H. Hiai.** 1988. Cloning and expression of the ret protooncogene encoding a tyrosine kinase with two potential transmembrane domains. Oncogene **3:**571–578.
36. **Takahashi, M., Y. Buma, and H. Hiai.** 1989. Isolation of the *ret* proto-oncogene cDNA with an amino-terminal signal sequence. Oncogene **4:**805–806.
37. **Takahashi, M., N. Asai, T. Iwashita, T. Isomura, and K. Miyazaki.** 1993. Characterization of the RET proto-oncogene products expressed in mouse L cells. Oncogene **6:**297–301.
38. **Treanor, J., L. Goodman, F. de Sauvage, D. M. Stone, K. T. Poulsen, C. D. Beck, C. Gray, M. P. Armanini, R. A. Pollock, F. Hefti, H. S. Phillips, A. Goddard, M. W. Moore, A. Buj-Bello, A. M. Davies, N. Asai, M. Takahashi, R. Vandlen, C. E. Henderson, and A. Rosenthal.** 1996. Characterization of a multicomponent receptor for GDNF. Nature **382:**80–83.
39. **Trupp, M., E. Arenas, M. Fainzilber, A. S. Nilsson, B. A. Sieber, M. Grigoriou, C. Kilkenny, E. S. Grueso, V. Pachnis, U. Arumae, H. Sariola, M. Saarma, and C. F. Ibanez.** 1996. Functional receptor for GDNF encoded by c-ret proto-oncogene. Nature **381:**785–789.
40. **Worby, C. A., Q. C. Vega, Y. Zhao, H. H. J. Chao, A. F. Seasholtz, and J. E. Dixon.** 1996. Glial cell line-derived neurotrophic factor signals through the RET receptor and activates mitogen-activated protein kinase. J. Biol. Chem. **271:**23619–23622.